

Original Research

ZNF429 Participates in the Progression of Coronary Heart Disease through Regulating Inflammatory and Adhesive Factors

Hao Wang^{1,*,†}, Bo Wu^{1,†}, Xueqin He¹, Wei Li¹, Wenqi Guan¹

Submitted: 30 April 2024 Revised: 28 May 2024 Accepted: 31 May 2024 Published: 24 September 2024

Abstract

Background: Coronary heart disease (CHD) is an intricate and multifaceted cardiovascular disorder that contributes significantly to global morbidity and mortality. Early and accurate identification and diagnosis of CHD are paramount to ensuring patients receive optimal therapeutic interventions and satisfactory outcomes. Methods: Data on CHD gene expression were obtained from the Gene Expression Omnibus (GEO) repository and potential hub genes were screened through gene ontology (GO), Kyoto Encyclopedia of Genes and Genomes (KEGG), weighted gene co-expression network analysis (WGCNA), and least absolute shrinkage and selection operator (LASSO) analyses. Functional validation of these hub genes was conducted by interfering with them in human umbilical vein endothelial cells (HUVECs). Cell proliferation and apoptosis were assessed through cell counting kit-8 (CCK-8) and flow cytometry assays, respectively, while enzyme-linked immunosorbent assay (ELISA), quantitative polymerase chain reaction (qPCR), Western blot, and immunofluorescence were used to measure the expression of key indicators. Results: We identified 700 upregulated differentially expressed genes (DEGs) and 638 downregulated DEGs in CHD, and utilized LASSO analyses to screen disease potential biomarkers, such as zinc finger protein 429 (ZNF429). Interference with ZNF429 in HUVECs mitigated the CHD-induced decrease in cell proliferation and increase in apoptosis. Moreover, the expression of interleukin-1 β (IL-1 β), interleukin-6 (IL-6), tumor necrosis factor-alpha (TNFα), vascular cell adhesion molecule-1 (VCAM-1), intercellular adhesion molecule-1 (ICAM-1), cluster of differentiation 62E (CD62E), and cluster of differentiation 62P (CD62P) was reduced, leading to decreased cellular inflammation and adhesion. Conclusions: CHDassociated biomarker ZNF429 was identified through bioinformatics analysis to potentially regulate the expression of inflammatory factors IL-6, IL-1β, and TNF-α, along with adhesion molecules ICAM-1, VCAM-1, CD62E, and CD62P. This modulation influence was subsequently found to impact the progression of CHD. These findings offered valuable insights into potential targets for further investigation and therapeutic interventions for CHD management.

Keywords: coronary heart disease; bioinformatics analysis; ZNF429

1. Introduction

Coronary heart disease (CHD), as a coronary artery disease and a prevalent cardiovascular ailment, is responsible for over 382,820 fatalities by 2023 [1]. Due to stenosis or occlusion of the coronary arteries due to coronary atherosclerosis, this disease is typically characterized by the amalgamation of plaque, lipid, cholesterol, and calcium sedimentation within coronary arteries, ultimately leading to myocardial ischemia, hypoxia, or cardiac necrosis [2]. Risk factors for CHD encompass high blood pressure, elevated cholesterol, tobacco use, obesity, diabetes, and genetic predisposition. Collectively, these factors expedite the onset of CHD, posing significant threats to the health of the elderly population [3]. Recently, the incidence of CHD shows that the group suffering from this disease tends to be younger and younger [4]. Most theoretical descriptions of the conceptual frameworks of CHD mechanisms, including spanning angina pectoris, myocardial infarction, ischemic cardiomyopathy, and occult CHD, are largely theoretical [5].

Despite recent advancements in the diagnosis of CHD, the identification of precise and sensitive biomarkers remains pivotal in managing this widespread disease. Studies have indicated that baseline levels and fluctuations in Btype natriuretic peptide and sensitive troponin I levels have the potential to guide the intensity of secondary CHD preventive therapies [6,7]. Further insights underscore serum uric acid (SUA) level as a prospective biomarker for CHD [8]. Elevated lipoprotein-associated phospholipase A2 levels have emerged as robust indicators of CHD risk, with implications for atherosclerosis and risk assessment [9]. While biomarkers and genes linked to CHD have been studied to enable early diagnosis, challenges persist in deciphering the functional significance of these biomarkers and genes, as well as their potential clinical utility. Thus, there is an urgent need to identify markers for early detection of CHD.

Increasing comprehensive gene expression profile databases have emerged due to gene expression analysis, providing valuable insights into diverse disease mecha-

¹Department of Cardiovascular, Yangpu Hospital, School of Medicine, Tongji University, 200090 Shanghai, China

^{*}Correspondence: 18916538685@163.com (Hao Wang)

[†]These authors contributed equally. Academic Editor: Natascia Tiso

nisms. Bioinformatics analysis is also a potent tool for unraveling the complex molecular mechanisms under the context of CHD development, as well as for identifying potential biomarkers and therapeutic targets [10,11]. This study employed bioinformatic analysis to identify CHD diagnostic biomarkers. Functional validation of the selected targets was conducted at the cellular level, providing valuable insights for advancing future diagnosis and targeted treatment of CHD.

2. Methods

2.1 Data Collection

Gene expression data for CHD and normal samples were retrieved from the Gene Expression Omnibus (GEO) database (https://www.ncbi.nlm.nih.gov/geo/query/acc.cgi?acc=GSE202625). The GSE202625 dataset, encompassing twenty-seven CHD blood samples and twenty-five normal blood samples, was used to validate the expression of potential marker genes.

2.2 Differential Expression Analysis

Differential expression analyses were conducted using the R package DESeq2 (1.38.3). Normalized data were assessed to identify differentially expressed genes (DEGs) between samples. Correction for multiple hypothesis testing was executed, and p-values were adjusted utilizing the false discovery rate (FDR), and the corrected p-value was called the q-value. DEGs were deemed statistically significant at a q-value < 0.05. The fold change (\log_2 FC) was calculated using fragments perkilobase of exon model per million mapped reads (FPKM) values, and DEGs with \log_2 FC >1 or \log_2 FC <-1 were considered up-regulated and downregulated, respectively.

2.3 GO and KEGG Enrichment Analyses

R software (R Foundation for Statistical Computing, Vienna, Austria), along with the "biological conductor" and "ggplot" packages (3.4.2), was employed for gene ontology (GO) function and Kyoto Encyclopedia of Genes and Genomes (KEGG) pathway enrichment analyses. The DEGs were categorized into biological processes, cellular components, and molecular functions. Enrichment was determined using an q-value of <0.05.

2.4 Weighted Correlation Network Analysis (WGCNA)

WGCNA explores genetic combinations and associations among samples, aiding biomarkers and therapeutic gene discovery [12]. The study employed 1338 DEGs to assess network topology for scale independence and connectivity using WGCNA. Hierarchical clustering was employed to cluster genes with comparable expression patterns into modules. Module—trait correlation identified highly CHD-associated module genes.

2.5 Screening Biomarkers by Constructing the LASSO Model

We assessed the impact of hub genes on CHD by employing a method of least absolute shrinkage and selection operator (LASSO) regression through the R glmnet [13]. LASSO is renowned for analyzing high-dimensional data, aiming to minimize the residual sum of squares while constraining the absolute sum of the model coefficients below a threshold. Genes with p < 0.05 significance were input into LASSO, yielding regression coefficients precisely equal to 0. This approach reduced data dimensionality by excluding low-weight variables and curbing overfitting due to covariate collinearity. We evaluated the diagnostic potential of these gene biomarkers by computing receiver operating characteristic (ROC) curves and measuring the corresponding area under the curve (AUC).

2.6 Cell Modeling and Grouping

Human umbilical vein endothelial cells (HU-VECs) (RRID: CVCL 2959, HTX2104) were obtained from Shenzhen OTWO Biotech Co., Ltd (Shenzhen, The cell lines were identified using short China). tandem repeat (STR) profiling, and the absence of mycoplasma contamination was confirmed. The sh-negative control (NC) plasmid and shZNF429 plasmid were designed and constructed by Chongqing Biomedicine Biotechnology Co., Ltd (Chongqing, China). The shZNF429 interference sequence is as follows: F-5'-GATCCGGCTATACAAAGGAGGTTATAACTCGAGTT ATAACCTCCTTTGTATAGCTTTTTTG-3'; AATTCAAAAAAGCTATACAAAGGAGGTTATAACTC GAGTTATAACCTCCTTTGTATAGCCG-3'. pLVX-shRNA1 vector without the insertion of the shZNF429 interference sequence serves as the NC. Specifically, two 1.5 mL EP tubes were prepared, with $25 \mu g$ NC plasmid added to the sh-NC group and $25 \mu g$ shZNF429 plasmid to the shZNF429 group. OPTI-MEM (31985070, GIBCO, Shanghai, China) was supplemented to make a final volume of 500 µL. Then, two additional 1.5 mL Eppendorf tubes (EP) were prepared by adding 75 µL transfection reagent max (24765-1, Biomedicine, Chongqing, China) and 425 µL optimized-minimal essential medium (OPTI-MEM) in each tube. After 5 minutes, the transfection reagent-containing mixture from the EP tubes was added into the plasmid-containing EP tubes, mixed thoroughly, let stand at room temperature for 15 minutes, and then added to HUVECs for passage and culture. The experimental groups were as follows: The control group: HUVEC cells were cultured in DMEM medium without serum and dual-antibody culture medium (C11995500BT, GIBCO, Shanghai, China). The model group: HUVEC cells were cultured in DMEM medium without serum and dual-antibody at a final concentration of 80 µg/mL oxidized low-density lipoprotein (ox-LDL, 20605ES05, Yeasen, Shanghai, China). The model+sh-NC



group: transfected sh-NC plasmid cell suspension was adjusted to a density of 2×10^5 cells/mL, and changed to culture in DMEM medium without serum and dual-antibody at a final concentration of $80~\mu g/mL$ ox-LDL. The model+shZNF429 group: transfected shZNF429 plasmid cell suspension was adjusted to a cell density of 2×10^5 cells/mL for plating, and cultured in DMEM medium without serum and dual-antibody at a final concentration of $80~\mu g/mL$ ox-LDL. After 24 h of culture in each group, samples were collected for subsequent detection. The gene level of ZNF429 was knocked down by transfection with shZNF429 plasmid. All experimental results were repeated three times.

2.7 Cell Counting Kit-8 (CCK-8)

Each well of a 96-well plate was supplied with $10~\mu L$ of CCK-8 solution (C0038, Beyotime, Shanghai, China). Blank wells were filled with culture medium and CCK-8 solution, while those for control with cells, culture medium, and CCK-8 solution. Following one-hour incubation, absorbance at 450 nm was measured using a microplate reader (CMax Plus, Molecular Devices, San Jose, CA, USA).

2.8 Flow Cytometry

For flow cytometry detection of cell proliferation, BeyoClick™ EdU-555 Cell Proliferation Kit (C0075S, Beyotime, Shanghai, China) was used following the operation steps. Cells were labeled with EdU, digested, resuspended, and added with 1 mL of 4% paraformaldehyde fixative solution. Following PBS treatment, 1 mL of permeabilization solution was supplied. Then, 0.5 mL of Click solution was added to each tube to evenly cover the samples, followed by incubation at room temperature for 30 minutes. The cells were detected using a flow cytometer (1026M, Betalco, Changzhou, China) and data were analyzed with FlowJo V10 software (FlowJo LLC, Ashland, OR, USA).

Flow cytometry apoptosis was detected using an Annexin V-FITC/PI apoptosis detection kit (40302ES60, Yeasen, Shanghai, China), following the manufacturer's protocol. After the collection of cell suspension from each group, the cells were centrifuged and the supernatant was discarded. The cells were gently resuspended with 195 μL of AnnexinV-FITC-A binding solution. Then, 5 μL of AnnexinV-FITC was added and mixed, followed by centrifugation and removal of the supernatant. Subsequently, 190 μL of AnnexinV-FITC-A binding solution was gently resuspended with cells. After adding the staining solution, the samples were placed in an ice bath in the dark before detection, and data were analyzed with FlowJo_V10 software.

2.9 Enzyme-Linked Immunosorbent Assay (ELISA)

ELISA experiments were conducted following the instructions provided with the respective assay kits. The ELISA kits for human IL-6, IL-1 β , and TNF- α were pur-

Table 1. Primer sequences.

| Primer name | Sequence |
|--------------------|-----------------------------|
| <i>ZNF429</i> -F | 5'-TTCTCTCTGGAGGAGTGGCA-3' |
| <i>ZNF429</i> -R | 5'-TCGCTTCATCTTGCAGGGTT-3' |
| VCAM-1-F | 5'-AGCACCACAGGCTCTTTTCC-3' |
| VCAM-1-R | 5'-ACACTTGACTGTGATCGGCTT-3' |
| ICAM-1-F | 5'-TGTGACCAGCCCAAGTTGTT-3' |
| ICAM-1-R | 5'-AGTCCAGTACACGGTGAGGA-3' |
| h- <i>GAPDH-</i> F | 5'-TCAAGGCTGAGAACGGGAAG-3' |
| h- <i>GAPDH-</i> R | 5'-CTCCTCCTCCTCCTGCTTCT-3' |
| | |

F, forward; R, reverse.

chased from Quanzhou Ruixinbio Co., Ltd (Quanzhou, China). The kits for intercellular adhesion molecule 1 (ICAM-1) and vascular cell adhesion molecule 1 (VCAM-1) were procured from Shanghai Qifa Laboratory Reagent Co., Ltd (Shanghai, China).

2.10 Quantitative Polymerase Chain Reaction (qPCR)

Total RNA was extracted from each cell group using the TRIzol method, and the concentration and purity of RNA were determined using a UV–visible spectrophotometer (OD260/OD280). Complementary DNA (cDNA) synthesis was performed using the cDNA synthesis kit instructions (TSK302M, Tsingke, Beijing, China), and the qPCR reaction system was prepared (TSE002, Tsingke, Beijing, China). Following this, reactions were conducted in a real-time fluorescent quantitative PCR instrument (Bio-Rad Laboratories, Hercules, CA, USA), with the housekeeping gene GAPDH employed for normalization. Gene expression levels were determined using the $2^{-\Delta\Delta Ct}$ method. Primer sequences can be found in Table 1.

2.11 Western Blot

The cell total protein was lysed on ice. In total, 500 μg of total protein from each sample was mixed with buffer (8015011, Dakewei, Shenzhen, China) (resulting in a protein concentration of approximately 3.3 μg/μL after mixing) and subjected to metal bath denaturation. Sixty micrograms of denatured protein were loaded for electrophoresis at 80 V until the samples entered the concentrating gel, followed by an increase in voltage to 120 V. Primary antibodies against ZNF429 (ab171422, abcam, Shanghai, China), VCAM-1 (A19131, abclonal, Wuhan, China), ICAM-1 (A20472, abclonal, Wuhan, China), and GAPDH (A19056, abclonal, Wuhan, China) were diluted at 1:1000 and incubated overnight at 4 °C. Secondary antibodies (AS014, abclonal, Wuhan, China) were then diluted at 1:2000 and incubated at room temperature for 1 hour. The membrane was uniformly covered with ECL exposure solution and detected using an exposure instrument (Universal Hood II, Bio-Rad, Hercules, CA, USA).



2.12 Immunofluorescence

Fixed cells were rinsed on the coverslip three times with PBS, each time for 5 minutes. After blocking with goat serum (C0265, Beyotime, Shanghai, China) for 30 minutes, primary antibodies against P-selectin (CD62P, 1:200, bs-0561R, Bioss, Beijing, China) and E-selectin (CD62E, 1:200, bs-1273R, Bioss, Beijing, China) were incubated at 4 °C overnight and washed three times. Secondary antibodies (1:200, GB21303, Servicebio, Wuhan, China) were added and incubated at room temperature for 1.5 hours and rinsed with PBS three times. DAPI staining (C1005, Beyotime, Shanghai, China) was performed, and the sections were sealed with an anti-fluorescence quenching agent (P0126, Beyotime, Shanghai, China) before observing changes under a microscope.

2.13 Data Statistics and Analysis

All experimental results were repeated three times. One-way ANOVA analysis and plotting were performed using Prism GraphPad 8.0 software (Dotmatics, Boston, MA, USA). Data display indicates mean \pm standard deviation (x \pm s), and p < 0.05 was considered statistically significant.

3. Results

3.1 ZNF429 Identified via Bioinformatics may be a Potential Biomarker for CHD

This study utilized the R DESeq2 package to identify 1338 genes with distinct expression patterns between normal and CHD samples ($|log_2FC| > 1$, q-value < 0.05). Within the set of 1338 DEGs, 700 genes were upregulated and 638 were downregulated (Fig. 1A). To screen for functional and pathway enrichments linked to CHDrelated DEGs, we conducted GO and KEGG enrichment analyses. GO analysis was employed to analyze the biological process (BP), cellular component (CC), and molecular function (MF) of the DEGs. GO analyses showed notable enrichment within specific biological processes, including leukocyte-mediated immunity and lymphocytemediated immunity. The chart displaying CC analysis revealed significant enrichment of DEGs within structures, such as the T-cell receptor complex, secretory granule membrane, and plasma membrane signaling receptor complex. In the MF category, DEGs demonstrated prominent enrichment in functions such as antigen binding, pattern recognition receptor activity, and immunoglobulin receptor binding (Fig. 1B). Regarding KEGG analysis, the outcomes demonstrated significant enrichment of DEGs in pathways including the ribosome, mitogen-activated protein kinase (MAPK) signaling pathway, coronavirus disease (COVID-19), ribosome biogenesis in eukaryotes, and the oxytocin signaling pathway (Fig. 1C).

By evaluating the scale-free topology fitting index for a specific power and network connectivity strength, we ensured alignment of the corresponding soft threshold power and a scale-free network. Network topology analysis was

used to determine a threshold force of 4, and a hierarchical clustering tree was generated based on this value (Fig. 1D,E). The resultant hierarchical clustering tree delineated 17 co-expressed gene modules that were identified for subsequent exploration. Further assessment addressed the independence among these 17 co-expression modules, revealing a minimal overlap between their constituent genes (Fig. 1F). Notably, the module-trait correlation heat map highlighted that the turquoise and brown modules had the highest correlations with CHD characteristics, with correlation coefficients of 0.80 (p = 0.0002) and 0.76 (p = 0.0006, Fig. 1G), respectively. Functional and pathway enrichment analyses were performed for DEGs within the turquoise and brown modules. The results of GO analysis highlighted predominant enrichment in key processes, such as regulation of protein ubiquitination, positive regulation of protein modification via small protein conjugation or removal, regulation of protein modification via small protein conjugation or removal, positive regulation of protein ubiquitination, ribosome, structural constituent of ribosome, and phosphatidylinositol bisphosphate phosphatase activity (Fig. 1H). KEGG analysis revealed substantial enrichment in pathways including the MAPK signaling pathway, signaling pathways regulating pluripotency of stem cells, the Hippo signaling pathway, Kaposi sarcoma-associated herpesvirus infection, and the ribosome (Fig. 1I).

LASSO analysis of DEGs from turquoise and brown modules was used to identify hub genes for CHD. Following LASSO analysis, the selection of these vital markers was accomplished through the precision of the penalty parameter adjustment, facilitated by a 10-fold cross-validation approach (Fig. 1J). LASSO regression analysis yielded two features, indicating that we reduced the number of latent variables to 2 (Fig. 1K). Consequently, two hub genes, SLC16A6 and ZNF429, demonstrated a discernible association with CHD. Subsequent ROC curve analysis further illuminated the discriminative potential of the logistic regression model based on these two marker genes. AUC values of SLC16A6 and ZNF429 were 0.952 and 0.984, respectively, underscoring the relatively high predictive efficacy of these hub genes in distinguishing between normal and CHD samples. This outcome underscores the considerable utility of the identified hub genes as potential indicators of CHD diagnosis and prediction (Fig. 1L). Based on the above analysis, we found that the AUC value of ZNF429 is higher. Therefore, ZNF429 was chosen for cell experimental validation.

3.2 Knockdown of ZNF429 Suppresses the Expression of Inflammatory and Adhesion Molecules

IL-6, IL-1 β , and TNF- α are common inflammatory cytokines, while VCAM-1 and ICAM-1 are adhesion molecules associated with CHD [14,15]. Previous studies have shown that *IL*-6, *IL*-1 β , *TNF*- α , *VCAM-1*, and *ICAM-1* levels are significantly increased in patients with



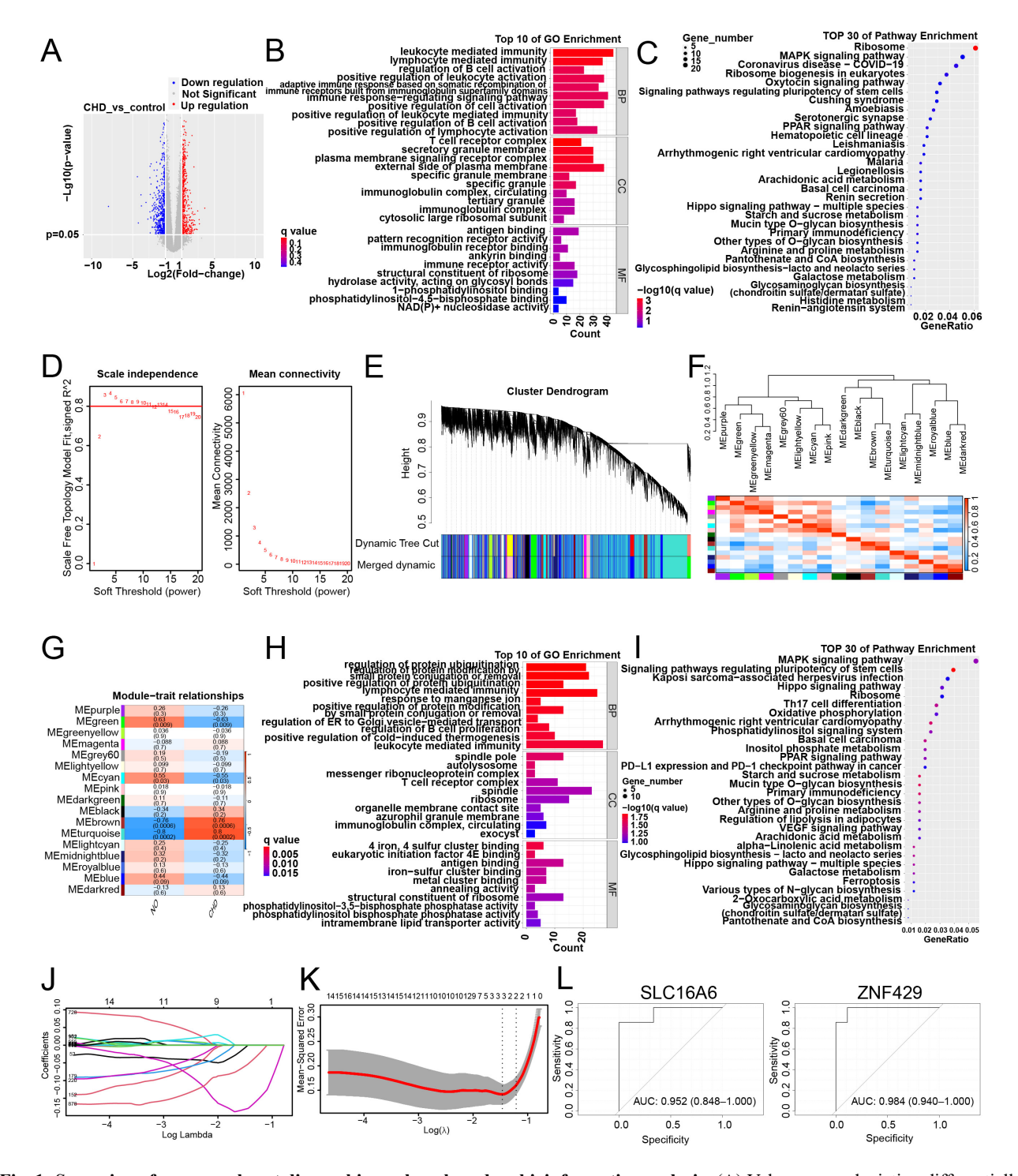


Fig. 1. Screening of coronary heart disease biomarkers based on bioinformatics analysis. (A) Volcano map depicting differentially expressed genes (DEGs) comparison between the coronary heart disease (CHD) group and control group, featuring distinctive color codes for gene expression alterations. (B) Top 10 gene ontology (GO) terms in the GSE202625 dataset. (C) Top 30 Kyoto Encyclopedia of Genes and Genomes (KEGG) pathways in the GSE202625 dataset. (D) The scale-free fitting index of soft threshold power. (E) Cluster dendrogram of DEGs using various metrics. Each branch signifies a gene, while colors below denote co-expression modules. (F) Interactions among co-expression modules. (G) Matrix illustrating the correlations and corresponding *p*-values between traits and modules. (H) Top 10 GO enrichment terms of DEGs within the turquoise and brown modules. (I) Top 30 KEGG enrichment pathways of the DEGs within the turquoise and brown modules. (J) Determination of the number of factors. (K) The important prognostic variables were selected using the least absolute shrinkage and selection operator (LASSO) regression method. (L) Logistic regression model to identify the area under the curve (AUC) of disease samples. The abscissa is the false positive rate, and the ordinate is the true positive rate.

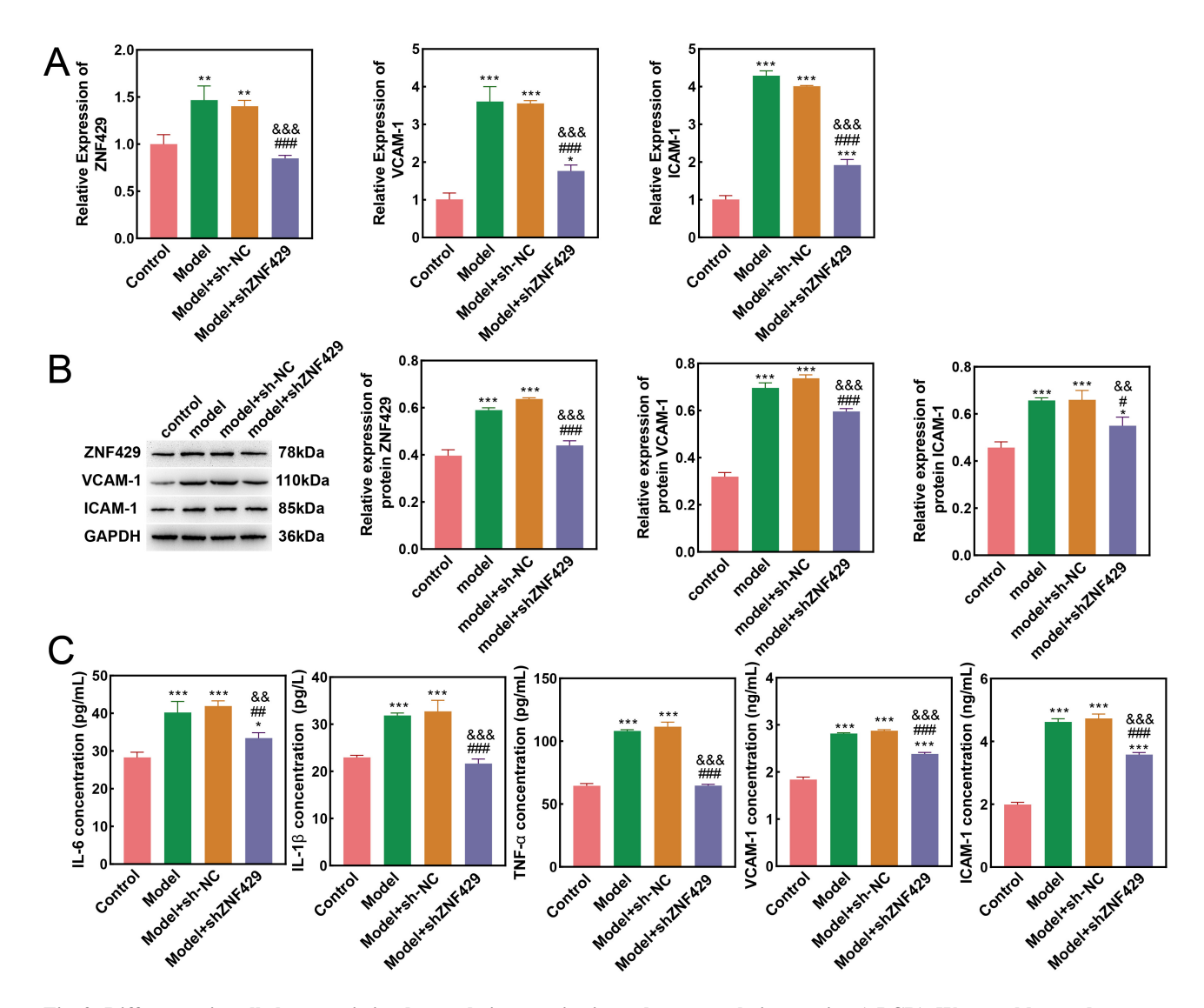


Fig. 2. Differences in cell characteristics detected via quantitative polymerase chain reaction (qPCR), Western blot, and enzymelinked immunosorbent assay (ELISA). (A) qPCR detection of the mRNA expression of ZNF429, VCAM-1, and ICAM-1 in cells. (B) Western blot detection of the mRNA expression of ZNF429, VCAM-1, and ICAM-1 in cells. (C) ELISA detection of IL-1 β , IL-6, TNF- α , VCAM-1, and ICAM-1 in the cells. Compared to control, *p < 0.05, **p < 0.01, *** p < 0.001. Compared to model, #p < 0.05, ### p < 0.01, ### p < 0.001. Compared to model+sh-NC group, && p < 0.01, &&& p < 0.001. n = 3.

CHD [16,17]. Based on bioinformatics analysis, we identified one hub gene, ZNF429. To further validate the roles of ZNF429 in CHD, we established a HUVEC cell model and interfered with ZNF429. In this study, qPCR detection results indicated that compared to control, mRNA expression levels of ZNF429, VCAM-1, and ICAM-1 were markedly increased in the model group and model+sh-NC group, confirming successful modeling (p < 0.01, p < 0.001). Furthermore, compared to the model, there was no significant difference in the mRNA expression of ZNF429, VCAM-1, and ICAM-1 in model+sh-NC (p > 0.05); in fact, they were greatly decreased in model+shZNF429 (p < 0.001). mRNA expression of ZNF429, VCAM-1, and ICAM-1 in model+shZNF429 decreased greatly vs. model and model+sh-NC groups (p < 0.001, Fig. 2A).

The Western blot analysis of the protein expression of ZNF429, VCAM-1, and ICAM-1 also exhibited a similar trend (Fig. 2B). ELISA results indicated significantly higher levels of IL-1 β , IL-6, TNF- α , VCAM-1, and ICAM-1 in the model group and model+sh-NC group compared to the control group (p < 0.001). In contrast, compared to the model+sh-NC group (p > 0.05), while the levels of IL-1 β , IL-6, TNF- α , VCAM-1, and ICAM-1 were significantly reduced in the model+shZNF429 group (p < 0.01, p < 0.001). The described factors in the model+shZNF429 group were greatly lower than those in the model+sh-NC group (p < 0.01, p < 0.01, p < 0.01, Fig. 2C). These results indicate that ZNF429 plays critical roles in regulating cell inflammation and adhesion.



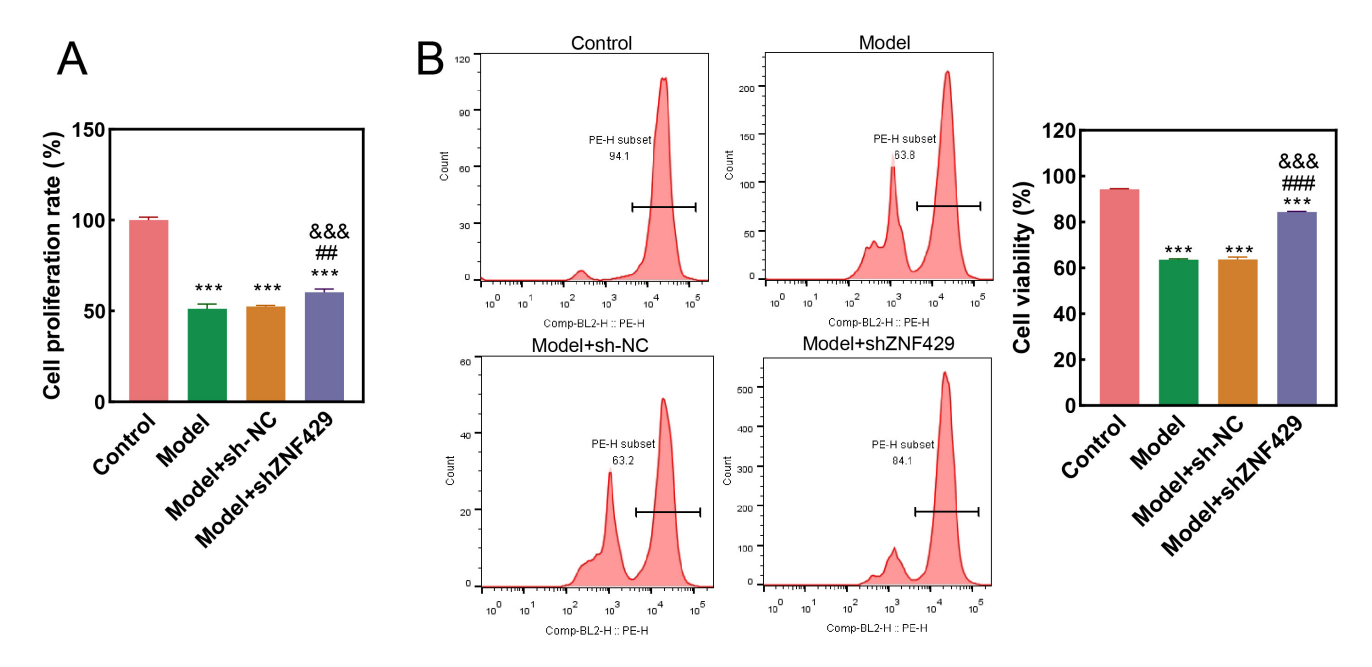


Fig. 3. Comparative analysis of cell proliferation in each group. (A) Cell proliferation detected via the cell counting kit-8 (CCK-8) assay. (B) Cell proliferation was evaluated via flow cytometry. PE-H subset: positive peak, indicating how many (%) proliferating cells were contained. Compared to control, *** p < 0.001. Compared to model, ## p < 0.01, ### p < 0.001. Compared to the model+sh-NC group, &&& p < 0.001. n = 3.

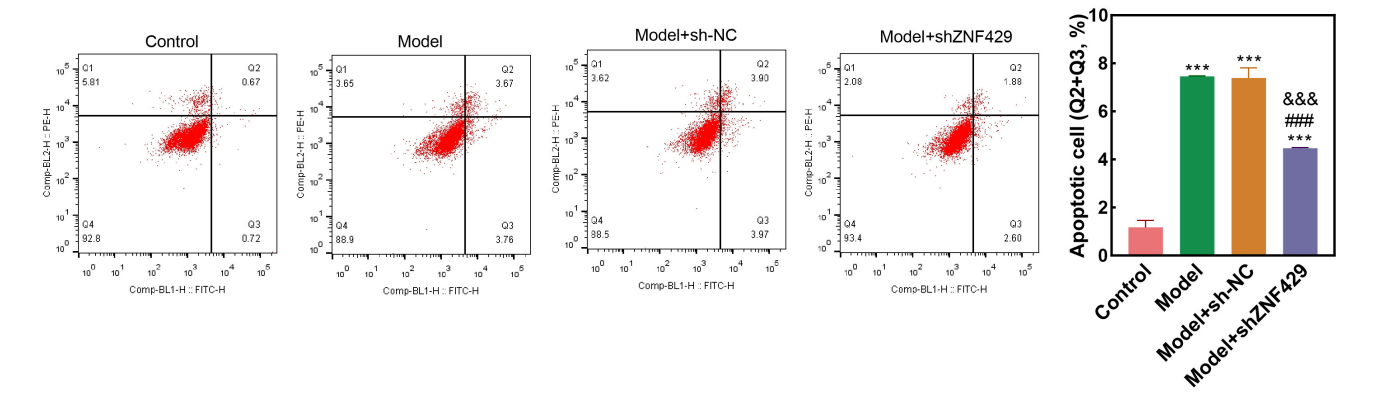


Fig. 4. Cell apoptosis detected through flow cytometry. Compared to control, *** p < 0.001. Compared to model, ### p < 0.001. Compared to the model+sh-NC group, &&& p < 0.001. n = 3.

3.3 Knockdown of ZNF429 Promotes Cell Proliferation and Inhibits Apoptosis

CCK-8 assay results demonstrated a significantly lower proliferation rate in the model group and model+sh-NC group compared to the control (p < 0.001). However, there were no significant differences in the model+sh-NC group and model group (p > 0.05). Notably, the model+shZNF429 group showed significant differences compared to both the model group and the model+sh-NC group ((p < 0.01, p < 0.001, Fig. 3A). The results of flow cytometry implied that compared with control, cell proliferation ability of model and model+sh-NC groups was greatly decreased (p < 0.001). Compared with the model group, there was no significant difference in the proliferation ability of the model+sh-NC group (p > 0.05), but the

proliferation ability of the model+shZNF429 group was notably increased (p < 0.001). In addition, the proliferation ability of model+shZNF429 was greatly higher than that of model+sh-NC (p < 0.001, Fig. 3B). Subsequently, we measured cell apoptosis. As shown in Fig. 4, compared with control, the apoptosis rate of model and model+sh-NC groups was significantly increased (p < 0.001). However, the model+shZNF429 group was significantly lower than the model and model+sh-NC groups (p < 0.01). These results indicated that interference with ZNF429 attenuated a decrease in cell proliferation rate but an increase in apoptosis rate caused by CHD.



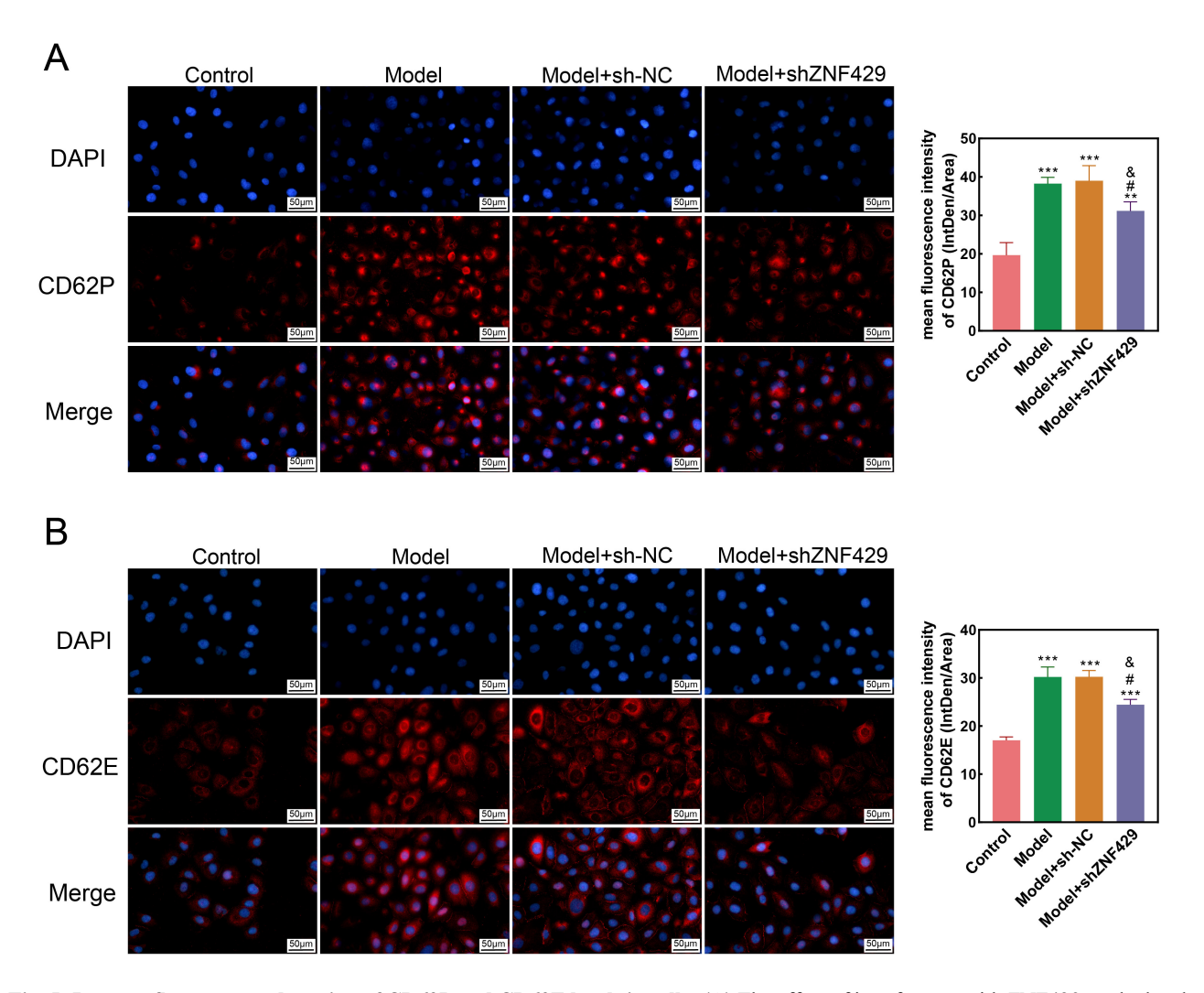


Fig. 5. Immunofluorescence detection of CD62P and CD62E levels in cells. (A) The effect of interference with ZNF429 on the levels of CD62P in each group (400×). (B) The effect of interference with ZNF429 on the levels of CD62E in each group (400×). Scale bar = 50 μ m. Compared to control, ** p < 0.01, *** p < 0.001. Compared to model, # p < 0.05. Compared to model+sh-NC, & p < 0.05. n = 3.

3.4 Knockdown of ZNF429 Reduces the Levels of CD62P and CD62E

CD62P and CD62E are selectins. Studies have found that CD62P is significantly elevated in patients with acute coronary syndrome [18–20], while CD62E plays an essential role in inflammation [21]. Therefore, we measured the levels of CD62P and CD62E after knocking down ZNF429. The immunofluorescence detection results are shown in Fig. 5. CD62P and CD62E levels in model and model+sh-NC groups were significantly increased vs control (p < 0.001). Compared with the model group, there was no significant difference in the model+sh-NC group (p > 0.05), but the levels of CD62P and CD62E in the model+shZNF429 group were greatly reduced (p < 0.05). Additionally, CD62P and CD62E levels in the model+shZNF429 group were substantially lower vs model+sh-NC (p < 0.05, Fig. 5A,B).

4. Discussion

CHD is a prevalent and global health concern due to high mortality in diverse age groups. Its pervasive impact places considerable strain on healthcare systems, in terms of both public health and economic implications [8]. New putative biomarkers are crucial for effective screening of CHD and primary prevention strategies. In this study, we utilized RNA sequencing-based gene expression analysis to identify potential biomarkers of congenital heart disease. Functional and pathway enrichment analyses of the DEGs revealed potential molecular mechanisms underlying CHD pathogenesis. GO enrichment analysis revealed significantly enriched processes such as leukocytemediated immunity, T-cell receptor complex, lymphocytemediated immunity, and antigen binding. KEGG analysis enriched pathways such as ribosome and MAPK signaling pathways. Employing WGCNA allowed the identification of gene modules with shared expression patterns, further re-



vealing hub genes within modules significantly associated with clinical features pertinent to the disease [22]. Of particular interest is that turquoise and brown modules had the highest correlation with CHD traits.

In this study, we identified two hub genes (SLC16A6 and ZNF429) through LASSO model analysis. The solute carrier 16 (SLC16) family is a group of membrane proteins that mediates the transmembrane transport of monocarboxylate complexes [23]. Alterations in the expression and transport of some SLC16 transporters can contribute to the occurrence of certain diseases, including cancer, diabetes, and neurological disorders [24]. Zinc finger proteins regulate DNA-dependent transcription frequency, rate, or extent. Despite its involvement in analgesic drug metabolism and pain pathways, the biological role of ZNF429 in CHD remains unclear. Identified within the turquoise and brown modules, these genes exhibited strong associations with CHD, extending their significance across diverse functions pertaining to CHD pathogenesis. These functions include the regulation of protein ubiquitination, ribosomes, phosphatidylinositol bisphosphate phosphatase activity, and eukaryotic translation initiation factor 4F complex. Therefore, we explored deeper into understanding the effect of ZNF429 on CHD.

Various inflammatory and adhesion molecules participate in the development of coronary artery atherosclerosis [25]. The factors IL-1 β , IL-6, and TNF- α have a significant impact on the occurrence of CHD [26,27]. Studies have shown that they can disrupt endothelial function and act on vascular wall plaques, accelerating plaque rupture and triggering clinical coronary artery events [28,29]. VCAM-1 and ICAM-1 are both adhesion molecules belonging to a family of immunoglobulin [30], expressed by endothelial cells. Their main function is to induce leukocytes to firmly adhere to endothelial cells, thereby promoting an increase in circulating levels of ICAM-1 and VCAM-1 [31]. Many studies have indicated that the polymorphisms of ICAM-1 and VCAM-1 are associated with myocardial infarction and coronary artery disease [32,33]. In this study, interference with ZNF429 alleviated the phenomenon of decreased cell proliferation rate and increased apoptosis rate caused by CHD. The expression of IL-1 β , TNF- α , IL-6, VCAM-1, and ICAM-1 was significantly reduced, reducing cellular inflammation and adhesion.

Prior research has demonstrated that factors CD62E, CD62P, ICAM-1, and VCAM-1 are elevated in patients with cerebral small vessel disease and arterial hypertension. These markers can be regarded as surrogates of endothelial expression [34,35]. Khanam *et al.* [36] have found that during the progression of the disease, cells produce inflammatory cytokines such as TNF- α , IL-6, and IL-10, which can induce the expression of adhesion molecules CD62E, CD106, and CD62P, leading to inflammation, endothelial damage, and plasma leakage. In this study, after interference with ZNF429, the levels of CD62E and CD62P were

reduced. We speculated that ZNF429 might regulate the expression of $TNF-\alpha$, IL-6, $IL-1\beta$, ICAM-1, and VCAM-1, which in turn regulated the expression of CD62E and CD62P, thereby influencing the progression of CHD. However, it is important to note that further investigations are warranted to elucidate the precise underlying mechanisms through which ZNF429 impacts disease characterization.

5. Conclusions

In summary, this study identified CHD-related biomarkers through bioinformatics analysis and validated them in HUVEC. These results indicate that ZNF429 regulates the progression of CHD by modulating the expression of $IL-1\beta$, IL-6, and $TNF-\alpha$, as well as adhesion molecules such as ICAM-1, VCAM-1, CD62E, and CD62P. These genes offer compelling avenues for a deeper exploration of CHD mechanisms. However, this study still has limitations. Specifically, we only verified the effects of ZNF429 in cells. Consequently, comprehensive in vitro and in vivo investigations are imperative for substantiating their functional relevance and effectiveness. Further research is needed to reveal the potential mechanisms of the key genes in the pathogenesis and recovery of CHD patients.

Availability of Data and Materials

The datasets used and analyzed during the current study are available from the corresponding author upon reasonable request.

Author Contributions

HW and BW performed most of the experiments, analyzed the data, and drafted the manuscript. XQH was mainly involved in data acquisition and article writing. WL and WQG interpreted the data and participated in article revision. HW participated in the project design and critically revised the manuscript. All authors contributed to editorial changes in the manuscript. All authors have contributed to and approved the final manuscript. All authors participated sufficiently in the work and agreed to be accountable for all aspects of the work.

Ethics Approval and Consent to Participate

Not applicable.

Acknowledgment

Not applicable.

Funding

This research received no external funding.

Conflict of Interest

The authors declare no conflict of interest.



References

- [1] Tsao CW, Aday AW, Almarzooq ZI, Anderson CAM, Arora P, Avery CL, *et al*. Heart Disease and Stroke Statistics-2023 Update: A Report From the American Heart Association. Circulation. 2023; 147: e93–e621.
- [2] Li N, Liu J, Ren Y, Cheng J. Diagnostic value of the cardiopulmonary exercise test in coronary artery disease. Journal of Thoracic Disease. 2022; 14: 607–613.
- [3] Ambrose JA, Singh M. Pathophysiology of coronary artery disease leading to acute coronary syndromes. F1000prime Reports. 2015; 7: 08.
- [4] Zhang H, Jing L, Zhai C, Xiang Q, Tian H, Hu H. Intestinal Flora Metabolite Trimethylamine Oxide Is Inextricably Linked to Coronary Heart Disease. Journal of Cardiovascular Pharmacology. 2023; 81: 175–182.
- [5] Dalen JE, Alpert JS, Goldberg RJ, Weinstein RS. The epidemic of the 20(th) century: coronary heart disease. The American Journal of Medicine. 2014; 127: 807–812.
- [6] Tonkin AM, Blankenberg S, Kirby A, Zeller T, Colquhoun DM, Funke-Kaiser A, et al. Biomarkers in stable coronary heart disease, their modulation and cardiovascular risk: The LIPID biomarker study. International Journal of Cardiology. 2015; 201: 499–507.
- [7] Wong YK, Tse HF. Circulating Biomarkers for Cardiovascular Disease Risk Prediction in Patients With Cardiovascular Disease. Frontiers in cardiovascular medicine. 2021; 8: 713191.
- [8] Uysal OK, Sahin DY, Duran M, Turkoglu C, Yildirim A, El-basan Z, et al. Association between uric acid and coronary collateral circulation in patients with stable coronary artery disease. Angiology. 2014; 65: 227–231.
- [9] Packard CJ, O'Reilly DS, Caslake MJ, McMahon AD, Ford I, Cooney J, et al. Lipoprotein-associated phospholipase A2 as an independent predictor of coronary heart disease. West of Scotland Coronary Prevention Study Group. The New England Journal of Medicine. 2000; 343: 1148–1155.
- [10] Gholipour A, Shakerian F, Zahedmehr A, Irani S, Malakootian M, Mowla SJ. Bioinformatics Analysis to Find Novel Biomarkers for Coronary Heart Disease. Iranian Journal of Public Health. 2022; 51: 1152–1160.
- [11] William C, Wangmo C, Ranjan A. Unravelling the application of machine learning in cancer biomarker discovery. Cancer Insight. 2023; 2: 1–8.
- [12] Langfelder P, Horvath S. WGCNA: an R package for weighted correlation network analysis. BMC Bioinformatics. 2008; 9: 559
- [13] Xiao S, Dong Y, Huang B, Jiang X. Predictive nomogram for coronary heart disease in patients with type 2 diabetes mellitus. Frontiers in Cardiovascular Medicine. 2022; 9: 1052547.
- [14] Amin MN, Siddiqui SA, Ibrahim M, Hakim ML, Ahammed MS, Kabir A, et al. Inflammatory cytokines in the pathogenesis of cardiovascular disease and cancer. SAGE Open Medicine. 2020; 8: 2050312120965752.
- [15] Cho YS, Kim CH, Ha TS, Lee SJ, Ahn HY. Ginsenoside rg2 inhibits lipopolysaccharide-induced adhesion molecule expression in human umbilical vein endothelial cell. The Korean Journal of Physiology & Pharmacology. 2013; 17: 133–137.
- [16] Han W, Wei Z, Zhang H, Geng C, Dang R, Yang M, et al. The Association Between Sortilin and Inflammation in Patients with Coronary Heart Disease. Journal of Inflammation Research. 2020; 13: 71–79.
- [17] Guo F, Sha Y, Hu B, Li G. Correlation of Long Non-coding RNA LncRNA-FA2H-2 With Inflammatory Markers in the Peripheral Blood of Patients With Coronary Heart Disease. Frontiers in Cardiovascular Medicine. 2021; 8: 682959.
- [18] Shen L, Yang T, Xia K, Yan Z, Tan J, Li L, *et al.* P-selectin (CD62P) and soluble TREM-like transcript-1 (sTLT-1) are asso-

- ciated with coronary artery disease: a case control study. BMC Cardiovascular Disorders. 2020; 20: 387.
- [19] Sakuma M, Tanaka A, Kotooka N, Hikichi Y, Toyoda S, Abe S, et al. Myeloid-related protein-8/14 in acute coronary syndrome. International Journal of Cardiology. 2017; 249: 25-31.
- [20] Seizer P, Fuchs C, Ungern-Sternberg SN, Heinzmann D, Langer H, Gawaz M, et al. Platelet-bound cyclophilin A in patients with stable coronary artery disease and acute myocardial infarction. Platelets. 2016; 27: 155–158.
- [21] Gupta GS. E-Selectin (CD62E) and Associated Adhesion Molecules. Animal Lectins: Form, Function and Clinical Applications (pp. 593–616). Springer: Vienna. 2012.
- [22] Dang R, Qu B, Guo K, Zhou S, Sun H, Wang W, et al. Weighted Co-Expression Network Analysis Identifies RNF181 as a Causal Gene of Coronary Artery Disease. Frontiers in Genetics. 2022; 12: 818813.
- [23] Bosshart PD, Charles RP, Garibsingh RAA, Schlessinger A, Fotiadis D. SLC16 Family: From Atomic Structure to Human Disease. Trends in Biochemical Sciences. 2021; 46: 28–40.
- [24] Felmlee MA, Jones RS, Rodriguez-Cruz V, Follman KE, Morris ME. Monocarboxylate Transporters (SLC16): Function, Regulation, and Role in Health and Disease. Pharmacological Reviews. 2020; 72: 466–485.
- [25] Christodoulidis G, Vittorio TJ, Fudim M, Lerakis S, Kosmas CE. Inflammation in coronary artery disease. Cardiology in Review. 2014; 22: 279–288.
- [26] Anderson DR, Poterucha JT, Mikuls TR, Duryee MJ, Garvin RP, Klassen LW, et al. IL-6 and its receptors in coronary artery disease and acute myocardial infarction. Cytokine. 2013; 62: 395– 400.
- [27] Mirhafez SR, Zarifian A, Ebrahimi M, Ali RFA, Avan A, Taj-fard M, et al. Relationship between serum cytokine and growth factor concentrations and coronary artery disease. Clinical Biochemistry. 2015; 48: 575–580.
- [28] Rajappa M, Sen SK, Sharma A. Role of pro-/anti-inflammatory cytokines and their correlation with established risk factors in South Indians with coronary artery disease. Angiology. 2009; 60: 419–426.
- [29] Ait-Oufella H, Libby P, Tedgui A. Anticytokine Immune Therapy and Atherothrombotic Cardiovascular Risk. Arteriosclerosis, Thrombosis, and Vascular Biology. 2019; 8: 1510-1519.
- [30] Fotis L, Agrogiannis G, Vlachos IS, Pantopoulou A, Margoni A, Kostaki M, et al. Intercellular adhesion molecule (ICAM)-1 and vascular cell adhesion molecule (VCAM)-1 at the early stages of atherosclerosis in a rat model. In Vivo. 2012; 26: 243–250.
- [31] Ley K. The role of selectins in inflammation and disease. Trends in Molecular Medicine. 2003; 9: 263–268.
- [32] Anbarasan C, Bavanilatha M, Latchumanadhas K, Ajit Mullasari S. ICAM-1 molecular mechanism and genome wide SNP's association studies. Indian Heart Journal. 2015; 67: 282–287.
- [33] Bielinski SJ, Pankow JS, Li N, Hsu FC, Adar SD, Jenny NS, et al. ICAM1 and VCAM1 polymorphisms, coronary artery calcium, and circulating levels of soluble ICAM-1: the multi-ethnic study of atherosclerosis (MESA). Atherosclerosis. 2008; 201: 339–344.
- [34] Sanada H, Midorikawa S, Yatabe J, Yatabe MS, Katoh T, Baba T, et al. Elevation of serum soluble E- and P-selectin in patients with hypertension is reversed by benidipine, a long-acting calcium channel blocker. Hypertension Research. 2005; 28: 871–878.
- [35] Zonneveld R, Martinelli R, Shapiro NI, Kuijpers TW, Plötz FB, Carman CV. Soluble adhesion molecules as markers for sepsis and the potential pathophysiological discrepancy in neonates, children and adults. Critical Care. 2014; 18: 204.
- [36] Khanam A, Gutiérrez-Barbosa H, Lyke KE, Chua JV. Immune-Mediated Pathogenesis in Dengue Virus Infection. Viruses. 2022; 14: 2575.

